# Elegant Ince–Gaussian breathers in strongly nonlocal nonlinear media*

Bai Zhi-Yong(白志勇), Deng Dong-Mei(邓冬梅), and Guo Qi(郭 旗)†

*Key Laboratory of Photonic Information Technology of Guangdong Higher Educaiton Institutes, South China Normal University, Guangzhou* 510631, *China*

(Received 31 August 2011; revised manuscript received 11 December 2011)

A novel class of optical breathers, called elegant Ince–Gaussian breathers, are presented in this paper. They are exact analytical solutions to Snyder and Mitchell's mode in an elliptic coordinate system, and their transverse structures are described by Ince-polynomials with complex arguments and a Gaussian function. We provide convincing evidence for the correctness of the solutions and the existence of the breathers via comparing the analytical solutions with numerical simulation of the nonlocal nonlinear Schrödinger equation.

**Keywords:** elegant Ince–Gaussian breathers, nonlocal nonlinear media

**PACS:** 42.65.Tg, 42.65.Jx **DOI:** 10.1088/1674-1056/21/6/064218

## 1. Introduction

Optical spatial solitons which are optical beams without change as they travel along the propagation axis in nonlinear media, exist when beams diffraction are balanced by nonlinearity. When the balance is broken, the characteristic width of the beams vibrates periodically, and optical spatial breathers occur.[1,2] The formation and dynamics of solitons and breathers in nonlocal nonlinear media are well described by the nonlocal nonlinear Schrödinger equation (NNLSE).[1,3,4] In 1997, Snyder and Mitchell[1] simplified the NNLSE to a simple linear model called the Snyder–Mitchell model (SMM) in strongly nonlocal nonlinear media (SNNM). This work stimulates people with a strong interest in studying the solitons and breathers in SNNM.[5−15]

Based on the SMM, standard Hermite–Gaussian beams,[8−10] Laguerre–Gaussian beams,[8,11,12] and Ince–Gaussian beams (IGBs)[13,14] have been obtained in Cartesian, cylindrical, and elliptic coordinates, respectively and they constitute three kinds of conventional complete families of exact analytic solutions of the SMM. These solutions all have the dynamics of solitons and breathers.

Besides the conventional solutions mentioned above, the SMM also has elegant solutions. The elegant Hermite–Gaussian[10] and elegant Laguerre–Gaussian[12] solutions of the SMM have been studied. However, the elegant Ince-Gaussian solutions of the SMM have not been reported.

In this paper, we are interested in introducing a novel class of exact elegant solutions to the SMM in an elliptic coordinate system. The solutions, called elegant Ince–Gaussian breathers (eIGBs), have much better symmetry than IGBs in mathematics, and are different from conventional IGBs in dynamics. The numerical simulation of the NNSLE agrees well with our conclusions.

## 2. Elegant Ince–Gaussian solutions of the SMM

The propagation of the optical beams in the nonlocal nonlinear cubic media can be described by the NNLSE

$$\mathrm{i}\frac{\partial\psi}{\partial z}+\mu\Delta_{\mathrm{T}}\psi-k\frac{\triangle n}{n_0}\psi=0, \tag{1}$$

where $\psi=\psi(\boldsymbol{r},z)$ is a paraxial beam, $\mu=1/2k$, $k=\omega n_0/c$ is the wave number in the media without nonlinearity, $n_0$ is the linear refractive index of the media, $\Delta_{\mathrm{T}}$ is the two-dimensional transverse Laplacian operator,

$$\triangle n=n_2\int R(\boldsymbol{r}-\boldsymbol{r'})|\psi(\boldsymbol{r'},z)|^2\,\mathrm{d}^2\boldsymbol{r'}$$

*Project supported by the National Natural Science Foundation of China (Grant Nos. 11074080 and 10904041), the Specialized Research Fund for the Doctoral Program of Higher Education of China (Grant No. 20094407110008), and the Natural Science Foundation of Guangdong Province of China (Grant No. 10151063101000017).

†Corresponding author. E-mail: guoq@scnu.edu.cn

© 2012 Chinese Physical Society and IOP Publishing Ltd

is the nonlinear perturbation of the refraction index, $n_2$ is the nonlinear index coefficient, $\boldsymbol{r}$ and $\boldsymbol{r'}$ are the two-dimensional transverse coordinate vectors, $z$ is the longitudinal coordinate, and $R(\boldsymbol{r}-\boldsymbol{r'})$ is the normalized symmetrical real spatial response function of the media.

For strong nonlocal nonlinear media, equation (1) can be simplified into the SMM[1]

$$\mathrm{i}\frac{\partial\psi}{\partial z}+\mu\Delta_{\mathrm{T}}\psi-\frac{n_2}{2n_0}k\gamma P_0 r^2\psi=0, \tag{2}$$

where $r=|\boldsymbol{r}|$ is the transverse distance from the beam center in the coordinate system, $\gamma$ is the material parameter which is related to the response function $R$, and

$$P_0=\int_{-\infty}^{+\infty}|\psi(\boldsymbol{r},0)|^2\,\mathrm{d}^2\boldsymbol{r}$$

is the input power at $z=0$.

To derive the elegant Ince–Gaussian solutions of the equation (2), we write them as multiplications of two functions:

$$\psi_{\mathrm{eIG}}=\psi_{\mathrm{eIn}}\psi_{\mathrm{G}}. \tag{3}$$

Inserting Eq. (3) into Eq (2), we obtain

$$\begin{aligned}&\psi_{\mathrm{G}}\left(\mathrm{i}\frac{\partial}{\partial z}+\mu\Delta_{\mathrm{T}}\right)\psi_{\mathrm{eIn}}\\&+2\mu\left(\frac{\partial\psi_{\mathrm{eIn}}}{\partial x}\frac{\partial\psi_{\mathrm{G}}}{\partial x}+\frac{\partial\psi_{\mathrm{eIn}}}{\partial y}\frac{\partial\psi_{\mathrm{G}}}{\partial y}\right)\\&+\psi_{\mathrm{eIn}}\left(\mathrm{i}\frac{\partial}{\partial z}+\mu\Delta_{\mathrm{T}}-\frac{n_2}{2n_0}k\gamma P_0 r^2\right)\psi_{\mathrm{G}}=0.\end{aligned} \tag{4}$$

Supposing

$$\left(\mathrm{i}\frac{\partial}{\partial z}+\mu\Delta_{\mathrm{T}}-\frac{n_2}{2n_0}k\gamma P_0 r^2\right)\psi_{\mathrm{G}}=0, \tag{5}$$

we can obtain from Eq. (4)

$$\begin{aligned}&\psi_{\mathrm{G}}\left(\mathrm{i}\frac{\partial}{\partial z}+\mu\Delta_{\mathrm{T}}\right)\psi_{\mathrm{eIn}}\\&+2\mu\left(\frac{\partial\psi_{\mathrm{eIn}}}{\partial x}\frac{\partial\psi_{\mathrm{G}}}{\partial x}+\frac{\partial\psi_{\mathrm{eIn}}}{\partial y}\frac{\partial\psi_{\mathrm{G}}}{\partial y}\right)=0.\end{aligned} \tag{6}$$

Equation (5) has the Gaussian-shaped solution[1,2,16]

$$\begin{aligned}\psi_{\mathrm{G}}(r,z)=&\frac{\sqrt{P_0}\exp[\mathrm{i}\theta(z)]}{\sqrt{\pi}w(z)}\\&\times\exp\left[-\frac{r^2}{2w(z)^2}+\mathrm{i}c(z)r^2\right],\end{aligned} \tag{7}$$

where $\theta(z)$ is the phase of the complex amplitude, $w(z)$ is beam width, and $c(z)$ is the phase-front curvature of the beam. These functions are given in Ref. [16] respectively

$$\theta(z)=-\arctan\left(\sqrt{P_c/P_0}\tan\beta_0 z\right), \tag{8a}$$

$$w(z)^2=w_0^2\left(\cos^2\beta_0 z+\frac{P_c}{P_0}\sin^2\beta_0 z\right), \tag{8b}$$

$$c(z)=\frac{\beta_0 k(P_c/P_0-1)\sin 2\beta_0 z}{\left(\cos^2\beta_0 z+\dfrac{P_c}{P_0}\sin^2\beta_0 z\right)}, \tag{8c}$$

where

$$\beta_0=\left(\frac{n_2}{n_0}\gamma P_0\right)^{1/2},$$

$w_0$ is the beam width at $z=0$, and

$$P_c=\frac{n_2}{\gamma w_0^4 k^2 n_0}$$

is the critical power of the Gaussian soliton.

Then, we solve Eq. (6) in an elliptic coordinate system. In a transverse $z$ plane, we define the complex elliptical variables as: $x=f(z)\cosh\xi\cos\eta$, $y=f(z)\sinh\xi\sin\eta$, where $(x,y,z)$ represent the real Cartesian coordinates, $\xi$ ($\xi\geq 0$) and $\eta$ ($0\leq\eta\leq 2\pi$) denote the radial and angular elliptic variables, and $f(z)=\sqrt{2\epsilon}\chi(z)$ which has the dimension of length is semifocal separation. In the expression of $f(z)$, $\epsilon=f_0^2/2w_0^2$ is the elliptic parameter, $f_0$ is the semifocal separation at waist plane $z=0$, and

$$\chi(z)=\sqrt{\frac{1}{2}w(z)^2[1+\mathrm{e}^{-2\mathrm{i}\theta(z)}]}.$$

When $z=0$, variables $(\xi,\eta)$ reduce to the real elliptical coordinates because of $\chi(0)=w_0$ and $f(0)=f_0$. Assuming

$$\psi_{\mathrm{eIn}}=A(z)E(\xi)N(\eta) \tag{9}$$

and inserting Eqs. (7) and (9) into Eq. (6), we can obtain the following separated equations

$$\begin{aligned}&\frac{\mathrm{d}^2E(\xi)}{\mathrm{d}\xi^2}-\epsilon\sinh 2\xi\frac{\mathrm{d}E(\xi)}{\mathrm{d}\xi}\\&\quad-(a-p\epsilon\cosh 2\xi)E(\xi)=0,\end{aligned} \tag{10}$$

$$\begin{aligned}&\frac{\mathrm{d}^2N(\eta)}{\mathrm{d}\eta^2}+\epsilon\sin 2\eta\frac{\mathrm{d}N(\eta)}{\mathrm{d}\eta}\\&\quad+(a-p\epsilon\cos 2\eta)N(\eta)=0,\end{aligned} \tag{11}$$

$$\mathrm{i}\chi(z)^2\frac{\mathrm{d}A(z)}{\mathrm{d}z}-\mu pA(z)=0, \tag{12}$$

where $A(z)$, $E(\xi)$, $N(\eta)$ are complex functions, and $p$ and $a$ are separation constants. Equation (12) can be solved easily

$$A(z)=\left[\frac{1+\mathrm{e}^{2\mathrm{i}\theta(z)}}{2}\right]^{p/2}. \tag{13}$$

Equation (11) is the Ince equation.[17−20] We note that equation (10) is equivalent to Eq. (11) via $\eta\mapsto\mathrm{i}\xi$. The solutions of Eq. (11) are known as the even and

odd Ince polynomials of order $p$ and degree $m$, usually expressed as $C_p^m$ and $S_p^m$, respectively, where $0 \leq m \leq p$ for even functions, $1 \leq m \leq p$ for odd function, and the indices $(p, m)$ have the same parity, i.e., $(-1)^{p-m} = 1$.

Equation (2) corresponds to the mathematical description of high-order eIGBs. To search for three-dimensional solutions, we combine the solutions of the same parity in $\xi$ and $\eta$ which are continuity in the whole space. Then, the elegant Ince Gaussian solutions can be obtained

$$\psi_{p,m}^{\mathrm{e}} = \frac{c_{pm}^{\mathrm{e}}}{w(z)} A(z) C_p^m(\mathrm{i}\xi, \epsilon) C_p^m(\eta, \epsilon) \times \exp\left[-\frac{r^2}{2w(z)^2} + \mathrm{i}c(z)r^2 + \mathrm{i}\theta(z)\right], \quad (14)$$

$$\psi_{p,m}^{\mathrm{o}} = \frac{s_{pm}^{\mathrm{o}}}{w(z)} A(z) S_p^m(\mathrm{i}\xi, \epsilon) S_p^m(\eta, \epsilon) \times \exp\left[-\frac{r^2}{2w(z)^2} + \mathrm{i}c(z)r^2 + \mathrm{i}\theta(z)\right], \quad (15)$$

where the superscript indices e and o denote even and odd modes, respectively, and $c_{pm}^{\mathrm{e}}$ and $s_{pm}^{\mathrm{o}}$ are normalization constants that are determined by

$$\int_{-\infty}^{+\infty} |\psi_{pm}^{\mathrm{e,o}}|^2 \mathrm{d}S = P_0,$$

$\mathrm{d}S$ is the area differential element across the transverse plane. At any $z$ plane, the $\psi_{p,m}^{\mathrm{e,o}}$ and its adjoint form $\widehat{\psi_{p',m'}}^{\mathrm{e',o'}}$ constitutes a biorthogonal set:

$$\int_{-\infty}^{+\infty} \psi_{p,m}^{\mathrm{e,o}} * \widehat{\psi_{p',m'}}^{\mathrm{e',o'}} \mathrm{d}S = \delta_{\mathrm{ee'},\mathrm{oo'}} \delta_{pp'} \delta_{mm'},$$

where $\delta$ is the Kronecker delta function.

## 3. Discussion of the solutions

As is known, due to the input power, the conventional Ince-Gaussian beams can be either solitons or breathers.[14]. But the elegant Ince–Gaussian beams have new dynamics. For the case of $p \neq 0$, because the modulation terms $\psi_{\mathrm{eIn}}$ is not constant, the transverse intensity distribution of the eIGBs is variable as the beams propagation along $z$ axis, and the period of the change is $z_R\pi$ for $P_0 = P_c$ and $z_R\pi\sqrt{P_c/P_0}$ for $P_0 \neq P_c$, where $z_R = kw_0^2$ is the Rayleigh range. The change of the transverse intensity distribution of the beams demonstrate the evolvement of the beams' width. The elegant Ince–Gaussian solutions only have breather states.

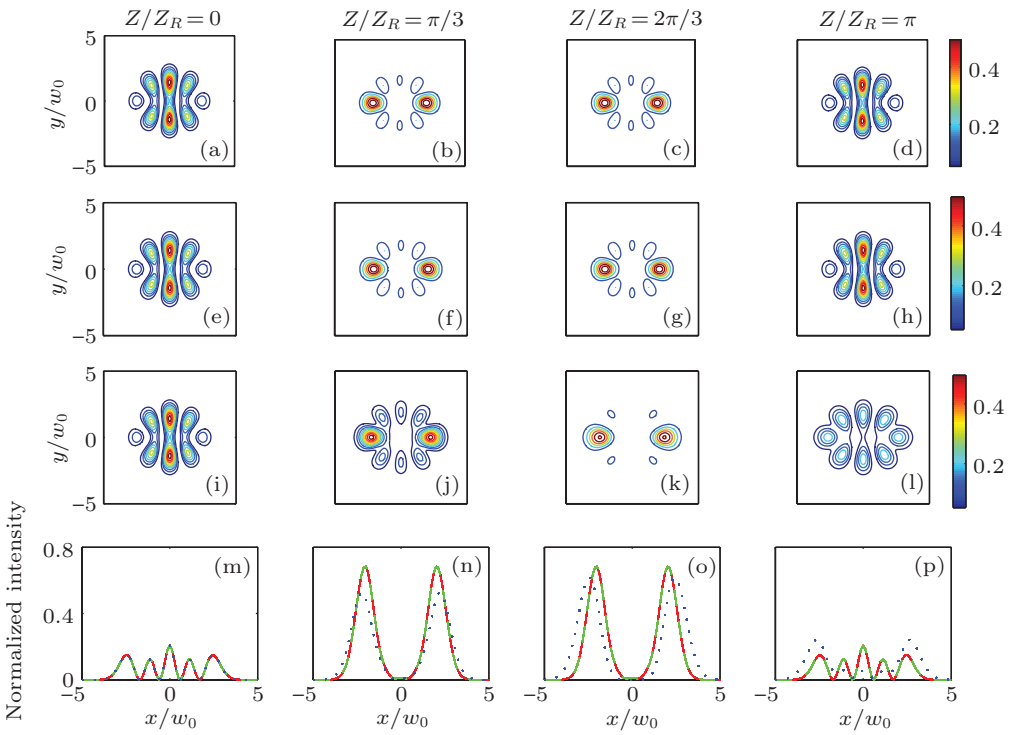



**Fig. 1.** (colour online) The dynamics of even mode eIGs with $p = 4$, $m = 4$, $\epsilon = 2$, $P_0/P_c = 1$. Panels 1(a)–1(d) are the transverse normalized intensity of the analytical solution. Panels 1(e)–1(h) show the transverse distribution of the numerical solution for $\alpha = 0.01$, and panels 1(i)–1(l) for $\alpha = 0.2$. Panels 1(m)–1(p) display the normalized intensity distributions at $y/w_0$, where the solid curves represents analytical solutions, and dashed and dotted curves are the numerical solutions for $\alpha = 0.01$, $\alpha = 0.2$. The different values of $z/z_R$ represent different propagation distances.

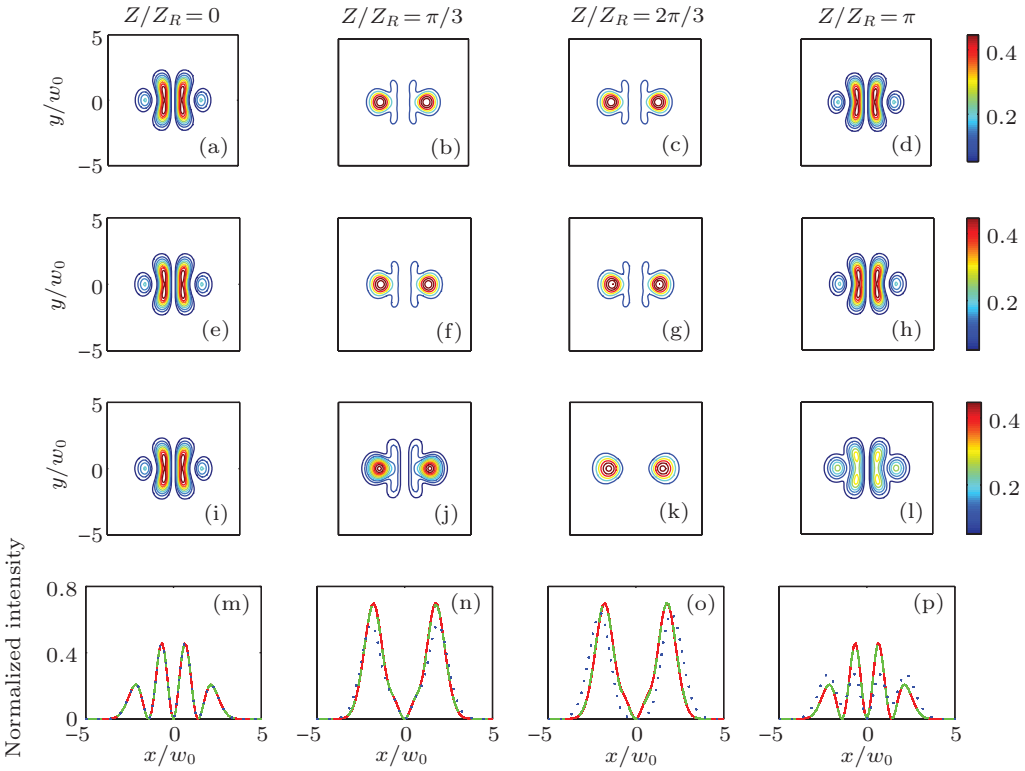



**Fig. 2.** (colour online) The behaviors of the dynamics for even mode eIGs are the same as those in Fig. 1 except for $p = 3$, $m = 3$, and $\alpha = 0.05$ in the second row.

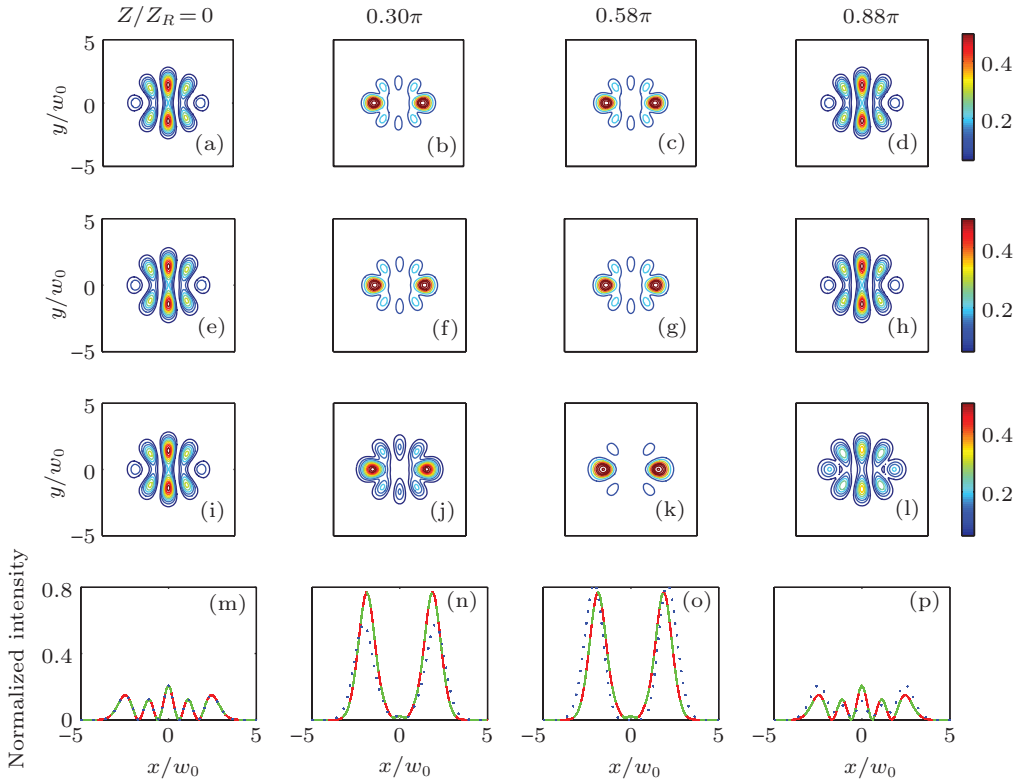



**Fig. 3.** (colour online) All behaviours are the same as those in Fig. 1 except $P_0 = 1.3P_c$.

If $p = 0$, equations (14) and (15) reduced to Eq. (7) which is the solution of the SMM for the (1+2)-dimensional case and can be regarded as the lowest-order elegant Ince–Gaussian solution. Depending on the input power, the beams have soliton and breather states. These can be affirmed by our numerical simulation.

To validate correctness of the solutions, the numerical simulation is presented. We set Eqs. (14) and (15) with $z = 0$ as input functions, and the material response is assumed to be a Gaussian function, i.e., $R(r) = 1/(2\pi w_m^2)\exp[-r^2/(2w_m^2)]$, here $w_m$ is the characteristic length of the material response. The parameter $\alpha = w_0'/w_m$, where $w_0'$ is the second order moment width of the input function, determines the degree of nonlocality. The smaller $\alpha$ is, the stronger the nonlocality. By applying the split-step Fourier method, we obtained the sketches of the three-dimensional field structure of eIGBs as shown in Figs. 1–4. The transverse field is sampled over a grid of $128 \times 128$.

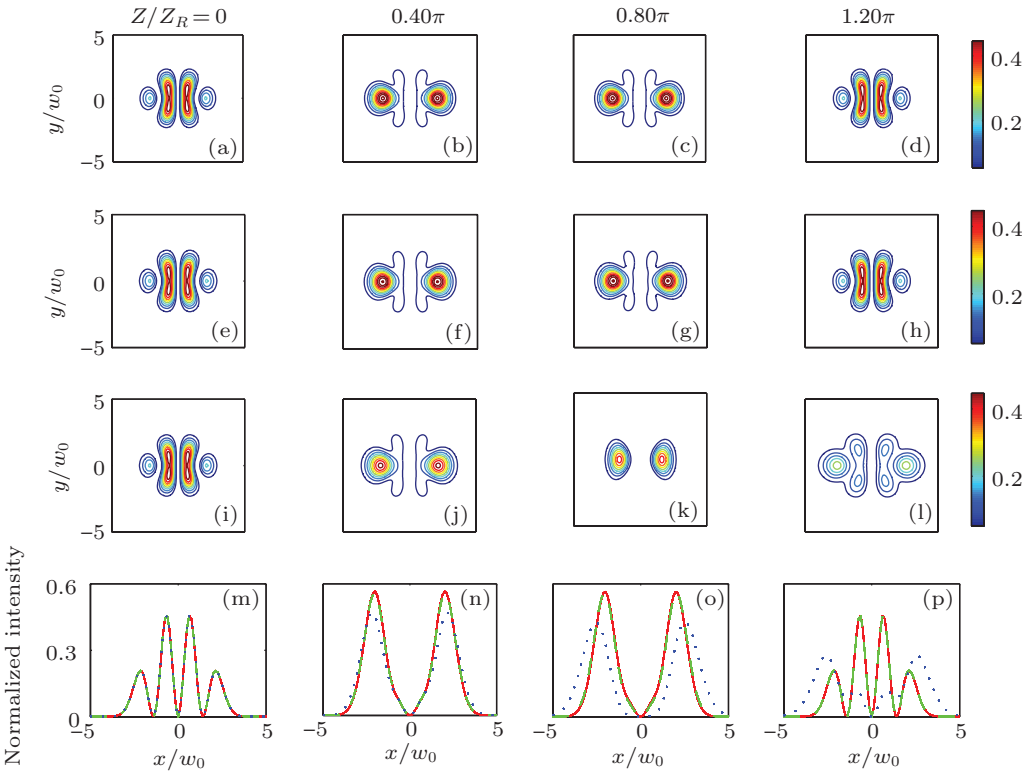



**Fig. 4.** (colour online) All are the same as those in Fig. 2 except $P_0 = 0.7P_c$.

From the figures, we can see that the transverse normalized intensity distributions of the optical beams periodically change as they travel along the $z$ axis. The period is $\pi$ for the case of $P_0 = P_c$ (Figs. 1 and 2), $0.88\pi$ for $P_0 = 1.3P_c$ (Fig. 3), and $1.20\pi$ for $P_0 = 0.7P_c$ (Fig. 4). The analytical solutions agree well with the numerical simulations when the degree of the nonlocality is very strong. As the degree of the nonlocality becomes weaker, the approximations of the analytical results to the numerical ones are a little worse, and when the degree of nonlocality is weak enough, they have great difference.

By studying the output normalized intensity distribution of the beams excited by an initial perturbation, we analyze the stability of eIGBs. We simulate the propagation of the beams once again, via assuming the normalized initial condition to be $A_0[\psi(\boldsymbol{r}) + \sigma\phi(\boldsymbol{r})]$, where $A_0$ is the amplitude of the beams, $\psi(\boldsymbol{r})$ is the normalized elegant Ince–Gaussian solution at $z = 0$, $\phi(\boldsymbol{r})$ is the random complex function whose maximum amplitude is less than 1 and $\sigma$ is the perturbation parameter, $\sigma\phi(\boldsymbol{r})$ represents a random perturbation. As $\sigma \to 0$, if the numerical results of the beams excited by an initial random noise tends toward that of the beams without perturbation, the solutions are stable. Figure 5 shows that the comparisons of the output normalized intensity distribution of the beams with different perturbation param-

eters. Compared with the solid lines, the dashed and dashed–dotted lines present a visible difference, but the dotted curves agree with them very well. Although the numerical stimulation is not rigorous proof of the stability, it does offer a strong support for the existence of observable nonlinear modes in lab experiments.

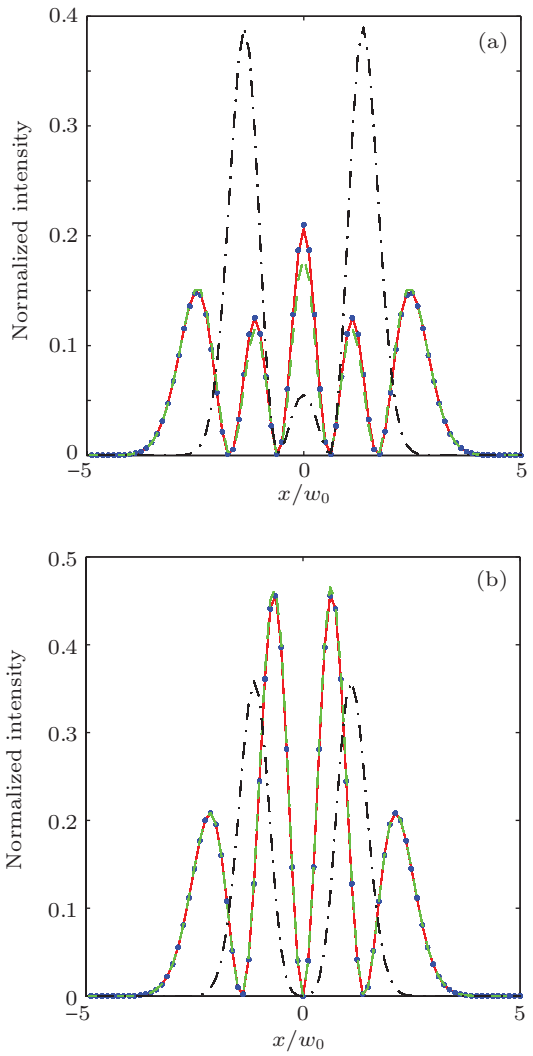



**Fig. 5.** (colour online) The comparisons of output normalized intensity distribution of the beams at $z = \pi z_R$: (a) (33) even eIG modes; (b) (44) even eIG modes. Different line types represent different perturbation parameters: solid lines for $\sigma = 0$; dotted lines for $\sigma = 0.001$; dashed lines for $\sigma = 0.01$; and dashed–dotted lines for $\sigma = 0.1$.

# 4. Conclusions

The exact elegant solutions of the SMM have been obtained in the SNNM in an elliptic coordinate. Because the beams only have the breather states for $p \geq 1$, the solutions whose transverse field distributions are described by the Ince polynomials with complex arguments and Gaussian function, are called elegant Ince–Gaussian breathers. The "breathing" period of the beams' width is measured by $z_R\pi\sqrt{P_c/P_0}$. The numerical simulation of NNLSE support our analysis well.

# References


[1] Snyder A W and Mitchell D J 1997 *Science* **276** 1538

[2] Guo Q, Luo B, Yi F, Chi S and Xie Y 2004 *Phys. Rev.* E **69** 016602

[3] Mitchell D J and Snyder A W 1999 *J. Opt. Soc. Am.* B **16** 236

[4] Krolikowski W, Bang O, Rasmussen J J and Wyller J 2001 *Phys. Rev.* E **64** 016612

[5] Conti C, Peccianti M and Assanto G 2003 *Phys. Rev. Lett.* **91** 073901

[6] Peccianti M, Dyadyusha A, Kaczmarek M and Assanto G 2006 *Nat. Phys.* **2** 737

[7] Rotschild C, Cohen O, Manela O, Segev M and Carmon T 2005 *Phys. Rev. Lett.* **95** 213904

[8] Buccoliero D, Desyatnikov A S, Krolikowski W and Kivshar Y S 2007 *Phys. Rev. Lett.* **98** 053901

[9] Deng D M, Zhao X, Guo Q and Lan S 2007 *J. Opt. Soc. Am.* B **24** 2537

[10] Deng D M and Guo Q 2010 *Eur. Phys. J.* D **60** 355

[11] Deng D M and Guo Q 2008 *J. Opt.* A: *Pure Appl. Opt.* **10** 035101

[12] Deng D M and Guo Q 2010 *Opt. Commun.* **283** 3777

[13] Deng D M and Guo Q 2007 *Opt. Lett.* **32** 3206

[14] Deng D M and Guo Q 2008 *J. Phys.* B: *At. Mol. Opt. Phys.* **41** 145401

[15] Deng D M and Guo Q 2009 *Phys. Rev.* A **79** 023803

[16] Guo Q 2004 *Proc. SPIE* **5281** 581

[17] Arscott F M 1964 *Periodic Differential Equations* (Oxford: Pergamon Press)

[18] Bandres M A and Gutiérrez-Vega J C 2004 *Opt. Lett.* **29** 144

[19] Bandres M A 2004 *Opt. Lett.* **29** 1724

[20] Bai Z Y, Deng D M and Guo Q 2011 *Chin. Phys.* B **20** 094202